

Heat Transfer in Beds of Fine Particles (Heat Transfer Perpendicular to Flow)

G. P. WILLHITE, DAIZO KUNII and J. M. SMITH

Northwestern University, Evanston, Illinois

Effective thermal conductivities were evaluated for beds of fine glass beads from experimental data on heat transfer perpendicular to the direction of fluid flow. Results were obtained for a bead size range of 29 to 940 μ and for carbon dioxide, nitrogen, helium, and a C_7 hydrocarbon liquid.

The results showed that over the range of flow rate studied 0 to 80 lb./ (hr. sq. ft.), or modified Reynolds number from 0 to 6.6, there was no effect of flow on the conductivity. Hence the measured stagnant conductivity k^0 , also satisfactorily represented heat transfer for flowing conditions. In view of this result, methods of predicting the stagnant conductivity were re-examined and a revised prediction method proposed. The equations are based upon a model which supposes energy to be transferred through a continuous fluid phase and through the solid particles by a solid-fluid series mechanism. The equations are compared with the data available in the literature.

In seeking an understanding of heat transfer in porous media a useful starting point is the problem of beds of small, spherical particles. There have been a number of studies (2, 3, 4, 6, 7, 8, 11, 12, 14) in beds in which the space surrounding the particles is filled with stagnant fluid. Kunii and Smith (5) summarized the previous work and proposed a model for heat transfer when the void space was filled with stationary fluid.

The practical goal of these studies is usually the solution of the problem of heat transfer in porous solids through which fluids are flowing. For example in thermal methods of petroleum recovery it is desirable to know the heat transfer characteristics of such materials as sandstones in which the pores are filled with flowing gases or liquids. The analogous, but simpler, case of beds of unconsolidated symmetrical particles is useful in developing a general understanding of heat transfer in porous media with fluid flow. In the range of particle sizes (1 to 1,000 μ) corresponding to porous rocks there have been very few studies. Kunii and Smith (6) measured heat transfer rates parallel to the direction of flow of fluid in beds of glass beads and sands. The results indicated that, even at low Reynolds numbers, the effective thermal conductivity k_e increased with the flow rate. This was explained on the basis of equations for the heat transfer coefficient between the fluid and particle.

The purpose of the present work is the study of heat transfer in beds of fine particles where the direction of heat flow is perpendicular to the fluid motion. In contrast to the parallel flow case the effective thermal conductivity was found to be independent of flow rate from 0 to 30 to 80 lb./ (hr.) (sq. ft.). Hence for perpendicular flow of energy and fluid it is only necessary to predict the stagnant fluid conductivity k^0 , in order to handle problems of heat transfer at moderate fluid velocities.

In view of these results the problem of predicting the stagnant conductivity was examined again and a new method proposed and compared with the available data.

SCOPE OF EXPERIMENTAL WORK

Measurements were carried out for six sizes of glass beads with four fluids, three gases and one hydrocarbon liquid (C_7 fraction). The description of the solid particles and the operating conditions are

summarized in Table 1. The gases used had the following purities:

Carbon dioxide (bone dry grade)	= 99.8%
Nitrogen (prepurified)	= 99.996%
Helium	= 99.995%

The hydrocarbon liquid had an analysis of 58.1 volume % paraffins, 39.7% naphthenes, and 2.2% aromatics, all primarily C_7 components. The complete analysis is available (9).

APPARATUS AND PROCEDURE

Figure 1 shows the entire apparatus and Figure 2 the details of the 2 in. I.D. cylinder used as the packed bed. The cylinder consisted of six, 3 in. long sections fitted together with flanges. A $\frac{3}{8}$ in. O.D. porcelain rod extended the length of the cylinder and was used as a support for the electrical heating ribbon. The heat generated at the rod passed radially through the bed of particles and was removed through the outer wall of the cylinder by cooling-water jackets.

The apparatus was used to measure heat transfer rates under both stagnant and flow conditions. For flow operation

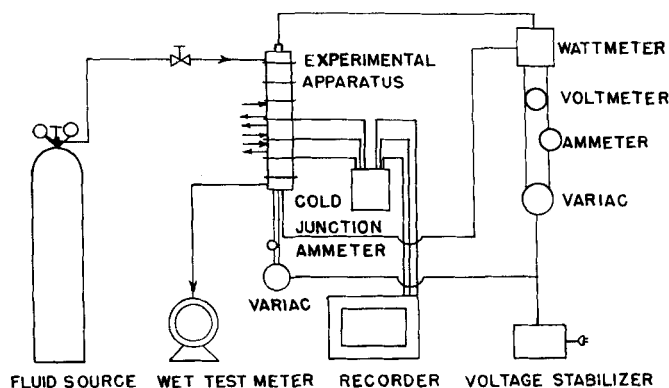


Fig. 1. Equipment layout.

G. P. Willhite is with Continental Oil Company, Ponca City, Oklahoma. Daizo Kunii is at the University of Tokyo, Tokyo, Japan. J. M. Smith is at the University of California, Davis, California.

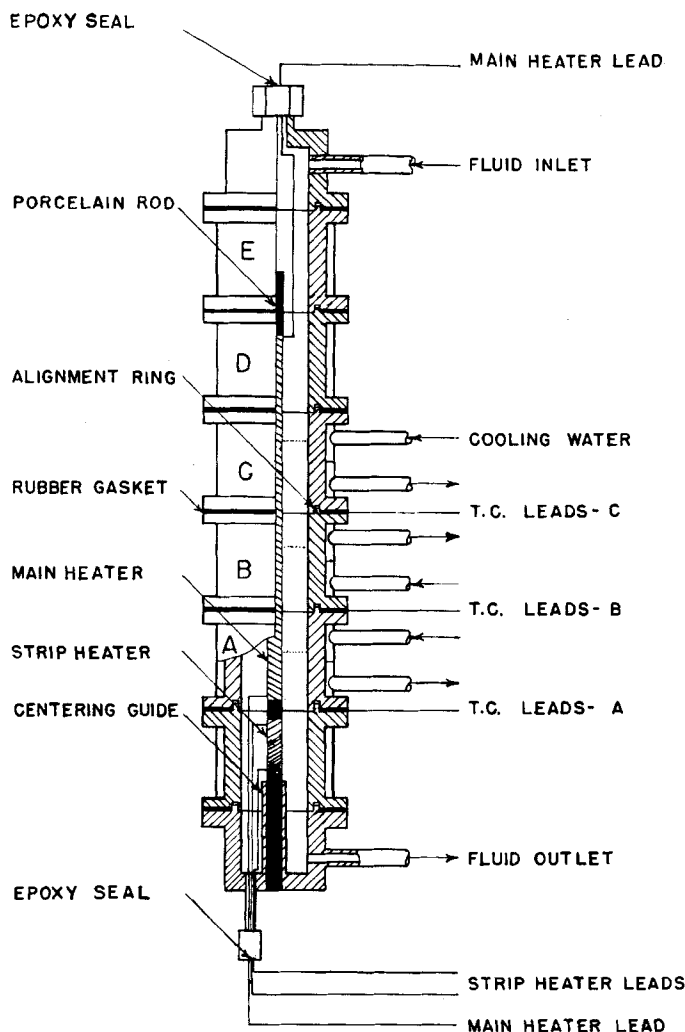


Fig. 2. Experimental apparatus.

the fluid entered the top and passed downward through packed sections D and E in order to obtain uniform velocity and temperature profiles. In sections A, B, and C a uniform radial temperature profile was established by generating heat at the center, and it was in these sections that the temperature measurements were made. The central test heater was prepared by wrapping Nichrome V ribbon around the porcelain rod for a length of 9 5/16 in. in sections A, B, and C. By careful wrapping it was possible to reduce variations in electrical resistance along the heater length to less than 2%. Since the axial temperature gradient near the center of the bed was small, the variation in resistance due to temperature changes was negligible. For these reasons it is believed that the rate of energy generation along the heater length was nearly uniform.

To insure that the flow of energy was in the radial direction, temperature profiles across the radius of the annular, packed bed were measured at three longitudinal positions, that is near the top of sections A, B, and C (see Figures 1 and 2). In order to maintain the same temperature profile at the three locations it was necessary to install a second heater 3/8 in. below the lower end of the test heater. This heater compensated for end

heat losses and bulk convection, and consisted of 30 gauge (B and S) Nichrome V wire wound for a length of 2 1/2 in. around the porcelain rod.

Temperatures at the three levels in the packed bed were determined with copper-constantan thermocouples prepared

from 36 gauge (B and S), nylon-insulated wire. Measurements were made at eight radial positions and at the wall. Support for the thermocouples consisted of two bamboo strips, 3/4 in. long and 1/16 in. square, between which the couples were cemented. This support extended across the radius of the tube in a horizontal direction as shown in Figure 2. The ends of the support were attached to the wall of the cylinder with epoxy resin. The junctions of the couples extended 3/4 in. upwards beyond the bamboo support to minimize the influence of the support on the temperature profile. This longitudinal run of the thermocouple leads and the use of 36 gauge wire tended to eliminate conduction errors in the temperature readings.

After the thermocouples were installed in the test cylinder, the locations of the junctions were adjusted to a definite distance from the wall by comparison with metal gauges. The eight gauges corresponded to the following distances from the cylinder wall: 0.095, 0.157, 0.254, 0.318, 0.402, 0.498, 0.630, and 0.751 in., within 0.001 in. The mean diameter of the thermocouple beads forming the junction was 0.017 in. Temperatures were measured to 0.5°F. The thermocouples were calibrated with the ice and steam points.

The glass beads used to pack the bed were supported on a wire screen. In the bottom section, where the compensating heater was located, graduated sizes of beads were used to prevent the smaller sizes of beads in the test section from blowing out. The test sections, A, B, and C were packed up to the level of the thermocouple junctions by tapping the section flange until settling of the beads could not be observed visually. The location of the thermocouples was adjusted as described in the previous paragraph. Then the section was completely filled in the same manner. The void fraction was measured from the mass of beads used to pack the test sections and the volume. The density of the beads was measured and found to vary slightly with size. The average value was 2.49 g./cc).

Flow rates of the gases were measured at atmospheric pressure with a wet test

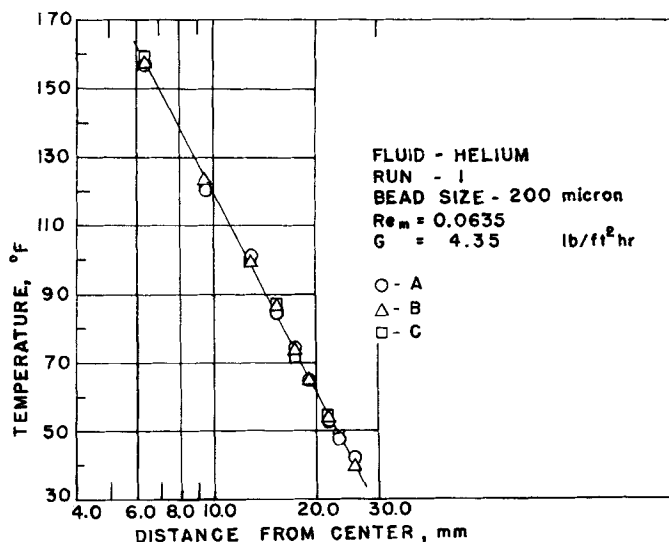


Fig. 3. Temperature profiles with strip heater.

TABLE 1. SCOPE OF DATA

Average diameter —microns	Glass beads k_s —Btu/(hr. ft. °F.)	Measured void Fraction of bed	Flow rate range lbs./ (hr. sq. ft.)	Reynolds no. Range— $D_p G/\mu$	Mean bed temp., °F. Gases** Liquid††
29*	0.605	0.37	0 to 33.8	0 to 0.089	90.2 72.7
66*	0.605	0.39	0 to 39.0	0 to 0.240	71.4 74.6
120*	0.605	0.37	0 to 41.7	0 to 0.470	67.4 72.6
200*	0.605	0.39	0 to 47.4	0 to 0.883	68.0 77.6
564†	0.605	0.37	0 to 59.8	0 to 3.11	80.0 64.3
940†	0.605	0.37	0 to 77.8	0 to 6.64	90.3 61.7

* From Minnesota Mining and Manufacturing Company who report experimental value of k_s = 0.605.

† From Potter Brothers, Inc., Carlstadt, New Jersey. Value of k_s is estimated.

** Gases: carbon dioxide, nitrogen, and helium.

†† Liquid Skellysolve C (estimated thermal conductivity 0.0815 B.t.u./(hr. ft. °F.) and viscosity 0.50 centipoises).

meter calibrated to 0.1%. Liquid flow rates were determined by gravimetric measurement to within 0.02 g./sec. The average pressure in the test section was 5 to 10 lb./sq. in. gauge for flowing-liquid runs and 0 to 10 lb./sq. in. gauge for stagnant runs with liquid. The pressure in the system with gases was near atmospheric. Small variations in pressure had no effect on the temperature profiles.

The power input to the test heater was measured within 0.05 w. (Total power input varied from 15 to 30 w.) It was necessary to use a voltage stabilizer to maintain a constant, 110 v. AC power source.

Measurements with and without the compensating heater showed that the profiles obtained in sections B and C were the same. However the temperatures in section A were lower unless the compensating heater was employed. With proper adjustment of this heater the temperatures at the three levels for any radial position agreed within 1.0°F., indicating that longitudinal heat flow had been reduced to small magnitudes. The data in Figure 3 for a test with 200- μ particles is typical of the temperature level and profiles observed.

Some preliminary measurements were made with upflow of fluid. The data for downflow and upflow showed no consistent differences, indicating that natural convection was not significant in the small pores.

RESULTS

Under steady state conditions, and assuming radial flow of the heat generated at the inner wall of the bed, the effective thermal conductivity is given by the equation

$$k_e = -\frac{Q}{\frac{2\pi L}{d \ln r} \frac{dT}{dr}} \quad (1)$$

The measured heater output Q and the temperature gradient are sufficient to evaluate k_e . Results for a specific run with a bed packed with 200- μ beads are shown in Figure 3. The linear plot indicates that the assumption [implied

in Equation (1)] of a constant k_s across the radius of the bed is satisfactory. There must exist a finite temperature difference between the solid and fluid temperature. However for fine particles this difference is very small, likely of the order of tenths of a degree or less. With the apparatus used here this difference was not detectable. The measured temperatures were probably close to the mean value of the particle and fluid temperature.

The experimental results in the form of effective thermal conductivities are shown for the four fluids in Figures 4 to 7. Measurements at the same conditions but different times indicated that the reproducibility of the data was always within 5%. This is somewhat larger than the estimated total error expected from the several experimental measurements.

Figures 4 to 7 show that within 5% (the precision of the data) there is no increase in k_e with flow rate. This suggests that heat transfer is by conduction and the effect of any turbulence

in the fluid is negligible. The introduction of turbulence in a packed bed is gradual as the flow rate increases. The slight increase in k_e in some of the data at the higher Reynolds numbers may be due to turbulence beginning to effect heat transfer perpendicular to flow. However over the whole flow range investigated the stagnant conductivity represents, within the precision of the data, the heat transfer characteristics of the bed. Perhaps this is not surprising in view of the very low Reynolds numbers involved. For example Singer (8a) has estimated the turbulent contribution to k_e by assuming a constant Pelet number of 4 and found this to be less than 0.01 at all conditions. However, the results are in contrast with previous work (6) on heat transfer parallel to the direction of fluid flow. For the same range of flow rates and for the same size glass beads the conductivity for parallel flow increased significantly with Reynolds number. It has been shown by measurements in packed beds that k_e in the parallel direction is eight to ten fold greater than the value for the perpendicular case. Such large differences are not evident in the data for fine particles reported here. The curves for parallel flow as measured by Kunii and Smith (6) start at the same point (the stagnant conductivity) as shown in Figures 4 to 7 and slope upwards for finite flow rates. The ratio of k_e in the parallel and perpendicular directions is thus unity at $Re_m = 0$ and increases with flow rate.

Figures 4 to 7 indicate also that the conductivity increases with particle diameter. The diameter increases thirty-two fold between the 29- and 940- μ beads, while k_e increased 20 to 25%.

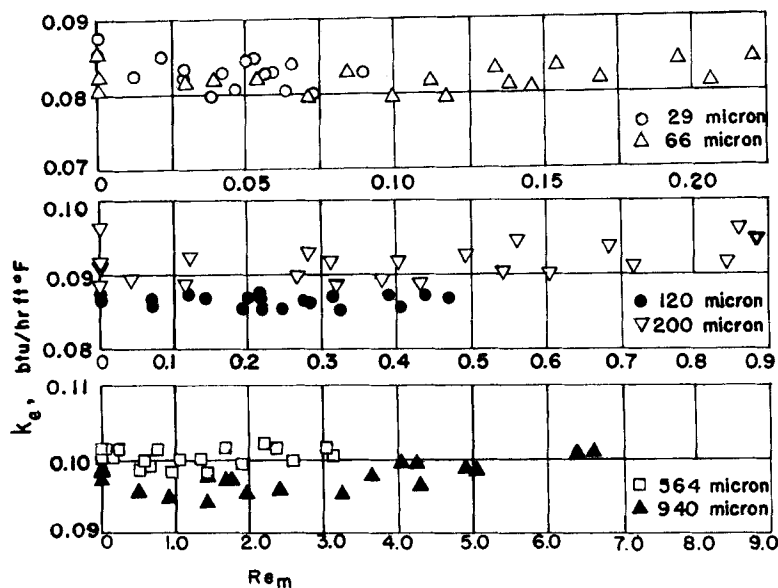


Fig. 4. Radial effective thermal conductivity data of carbon dioxide runs.

Hence the effect is small, but greater than the precision of the data.

PREDICTION OF STAGNANT CONDUCTIVITY

The equations for stagnant conductivity k° , developed in reference (5), considered energy to be transferred by two means: (1) through the void fraction of the bed by conduction and radiation, and (2) through a series path consisting of an equivalent thickness l_s of solid and an equivalent thickness l_v of fluid between the solid particles. In parallel with the fluid resistance are radiation and solid-to-solid contact resistances. This model of the heat transfer process was illustrated in Figure 1 of reference 5.

That the concepts employed were generally sound was indicated by reasonable agreement with most of the experimental data. However further analysis of the equations for beds of spherical particles at relatively low temperatures has suggested improvements. At these conditions heat transfer by radiation and by point contact from particle to particle is negligible and Equation (3) of reference 5 is applicable. This expression is

$$\frac{k^\circ}{k_g} = \epsilon + \frac{(\gamma + \phi)(1 - \epsilon)}{\phi + \gamma \left(\frac{k_g}{k_s} \right)} \quad (2)$$

With these restrictions the packed bed may be replaced by a two-dimensional model as shown in Figure 8. Here the distance ΔL is the thickness of an individual element which is repeated throughout the bed and which represents the sum of the thicknesses l_s and of the equivalent solid and fluid

spaces in the nonvoid section of the model. In Equation (2) $\gamma = l_s/D_p$ and $\phi = l_v/D_p$.

Equation (2), based upon ϵ as the actual void fraction, is not exactly cor-

The expression developed (5) for α involves the number of contact points n between the hemispherical surface of a particle and adjoining particles. It is given by

$$\alpha = \frac{1}{2n} \frac{\left(\frac{k_s - k_g}{k_s} \right)^2 \sin^2 \theta_o}{\text{Ln} \left[\frac{k_s}{k_g} - \left(\frac{k_s}{k_g} - 1 \right) \cos \theta_o \right] - \frac{k_s - k_g}{k_s} (1 - \cos \theta_o)} \quad (5)$$

rect. This is because part of the nonvoid section is void, namely the fraction $l_v/(l_s + l_v)$. A consistent representation would be to divide the model into a so-called void section ϵ^* , and a so-called nonvoid section $1 - \epsilon^*$. Then in Equation (2) the proper value of the void fraction to use is ϵ^* , rather than the actual value ϵ . The relationship between the two is

$$\epsilon^* = \frac{\epsilon - \frac{\phi}{\phi + \gamma}}{1 - \frac{\phi}{\phi + \gamma}} \quad (3)$$

The determination of ϕ leads to an equation which involves the sum $\phi + \gamma \frac{k_g}{k_s}$. If this sum is defined as α , and if Equation (2) is written in terms of ϵ^* rather than ϵ

$$\frac{k^\circ}{k_g} = \epsilon^* + (1 - \epsilon^*) \frac{\alpha + \gamma \left(1 - \frac{k_g}{k_s} \right)}{\alpha} \quad (4)$$

The angle θ_o is related to the number of contact points by the equation

$$\frac{1}{n} = \sin^2 \theta_o \quad (6)$$

In the original development the number of contact points was related to the geometry of packing of spherical particles, and then an empirical scheme was used to obtain an average value of α from the void fraction. However Foote, Smith, and Busang (10) have studied in detail the number of contact points in beds of spherical particles. Their theoretical results agreed well with direct experimental measurement of number of contact points and led to the following equation between void fraction and n :

$$n = (3) \frac{5.01 - 8.42\epsilon}{1.91 - 1.91\epsilon} \quad (7)$$

Equations (5) to (7) permit the determination of α from the void fraction of the bed. Combination of Equations (3) and (4) along with the definition of α gives the following relationship for k°/k_g in terms of α and γ :

$$\frac{k^\circ}{k_g} = 1 + (1 - \epsilon) \left(1 - \frac{k_g}{k_s} \right) + \frac{\gamma}{\alpha} \left(1 - \frac{k_g}{k_s} \right)^2 (1 - \epsilon) \quad (8)$$

Equation (8) may be used to predict the stagnant conductivity from the void fraction, k_g/k_s , and γ . The original expression [Equation (3) of reference 5] contained a second parameter in addition to γ .

The quantity γ is proportional to the equivalent length of the path (l_s) for heat transfer through a given spherical particle by conduction. For a single contact point the path length would be twice the distance from the point of contact to the particular diameter of the sphere which is perpendicular to the overall direction of heat transfer. The equivalent length will be proportional to the average of such distances for all the contact points on the hemispherical surface of the given sphere. It is clear that the maximum value of the distance for a single contact point

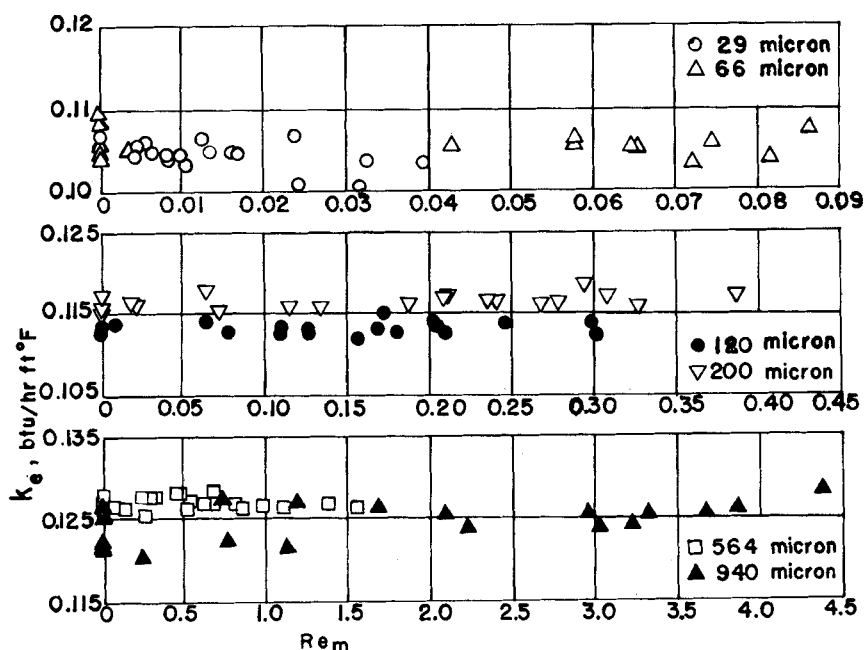


Fig. 5. Radial effective thermal conductivity data of nitrogen runs.

is $D_p/2$, so that the path length would be D_p , or $\gamma = 1$. Since the minimum distance would be zero ($\gamma = 0$), the average value of γ will be of the order of $1/2$.

The experimental data of this investigation were found to correlate well with Equation (8) using a value of $\gamma = 2/3$. The average deviation of the twenty-four points of k° , obtained from Figures 4 to 7 was 6.8%. Figure 9 compares all the available experimental data for stagnant thermal conductivity with calculated results using Equation (8). The range of particles included in Figure 9 are given in Table 2. The fluids employed by the several investigators included gases (carbon dioxide, air, nitrogen, helium, hydrogen, methane, and propane) and liquids (water, glycerine, iso-octane, and ethyl alcohol). When one considers the wide range of solids and fluids, the agreement indicated in Figure 9 is good. The computed values of k° for nonspherical particles were based upon a value of $\gamma = 1/2$ in order to improve the agreement with the experimental data. Equation (8) was derived for spherical particles, and the need for a lower value of γ may represent a correction for deviation from spherical shape. Also the computed results for spherical particles of high conductivity, that is lead or steel, are based upon $\gamma = 1/2$.

The corrected void fraction ϵ^* must be positive. From Equation (3) it is seen that this requirement will be met when

$$\frac{\phi}{\phi + \gamma} < \epsilon \quad (9)$$

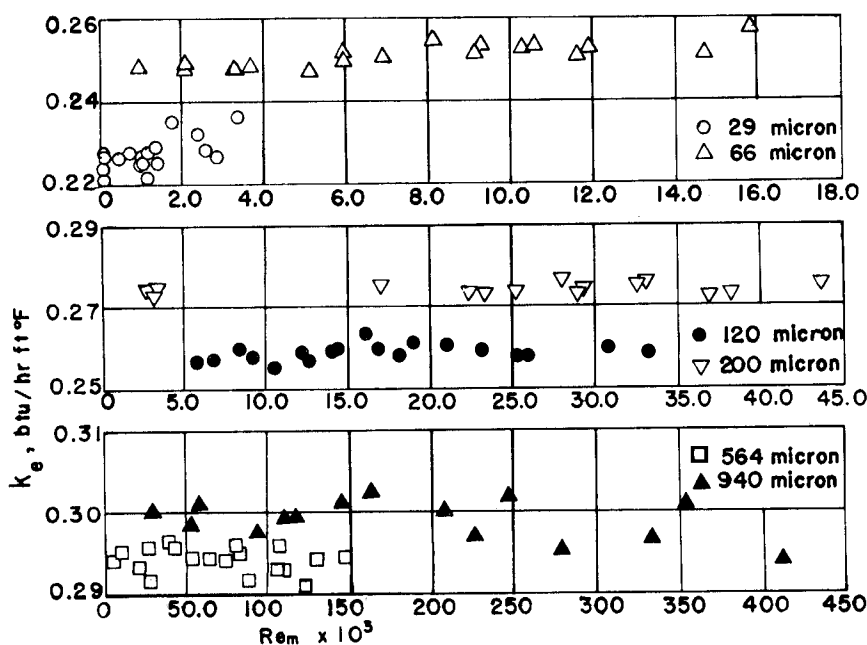


Fig. 6. Radial effective thermal conductivity data of helium runs.

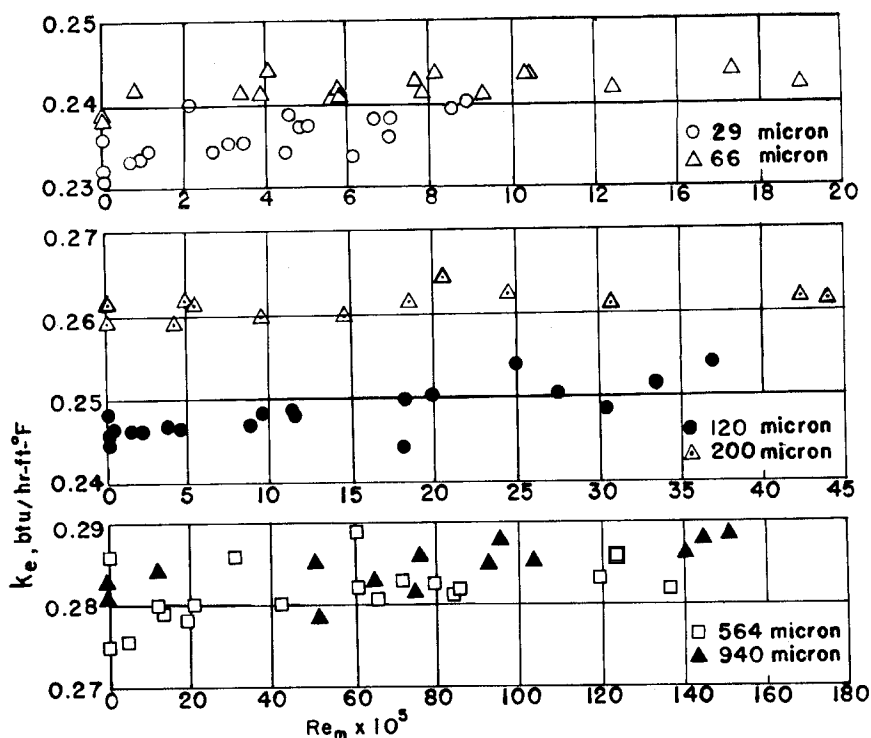


Fig. 7. Radial effective thermal conductivity data of skellysolve C runs.

This restriction is satisfied if ϕ is less than $1/3$ for $\epsilon = 0.40$ and $\gamma = 1/2$. Equations (5) to (7) indicate that this will be the case if k_s/k_g is greater than about 1.0. In other words Equation (8) would be applicable to most fluid-solid systems but, for example, would not be satisfactory for a mercury-glass bead system where k_s/k_g is about 0.1.

It is of interest to compare the data obtained in this study with previous prediction methods. Eucken (1) pro-

posed a simple theoretical equation relating the stagnant conductivity to k_s , and the void fraction. The equation correctly showed the influence of some of the variables but did not predict well the magnitude of k° . Schumann and Voss (8) presented more sophisticated equations containing a single parameter. When these equations are applied to the data in Figures 4 to 7, the average absolute deviation is 17.8% vs. 6.8% with Equation (8).

Wilhelm and colleagues (13) made a statistical analysis of the deviation of the available data from Schumann and Voss's equations and proposed a correction term. This corrected version of the Schumann and Voss approach showed an average deviation of 12.9% from the information in Figures 4 to 7. Preston (7) found it necessary to apply a different correction procedure to the Schumann and Voss approach to obtain agreement with his data. This modified procedure gave an average deviation of 12.5% compared with the data in Figures 4 to 7.

In summary a method has been proposed for predicting the stagnant con-

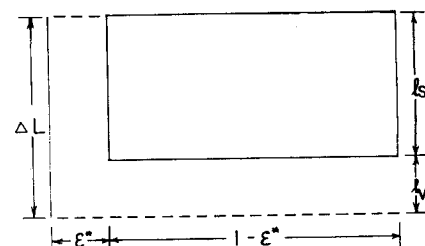


Fig. 8. Model of element of bed.

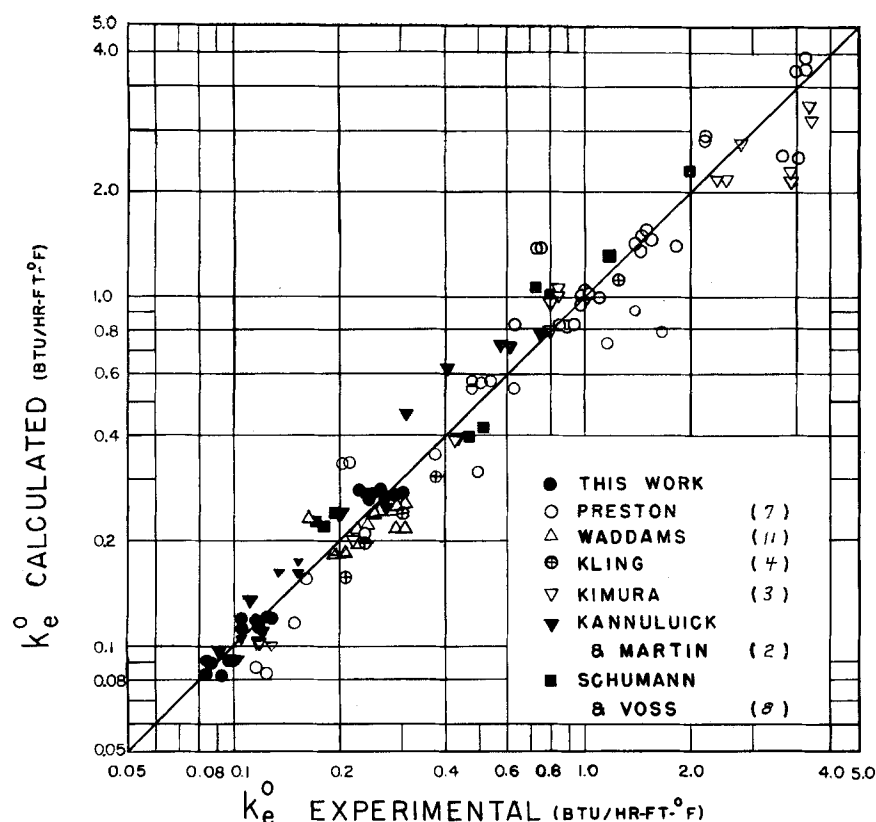


Fig. 9. Comparison of Equation (8) and experimental k_e^0 .

ductivity in beds of spherical particles which agrees better than previous methods with the data obtained in this study. The method also has been applied to all the previous experimental data as shown in Figure 9. Even though some of the information was for non-spherical particles, the calculated results agree with the data with an average absolute deviation of 15%.

ACKNOWLEDGMENT

The technical and financial assistance of the California Research Corporation,

Petroleum Research Fund (American Chemical Society), and Socony Mobil Oil Company is gratefully acknowledged.

NOTATION

- D_p = diameter of particles in packed bed, ft.
 k_e^0 = stagnant thermal conductivity, B.t.u./ (hr.ft. °F.)
 k_e = effective thermal conductivity with flowing fluid, B.t.u./ (hr. ft. °F.)
 k_s = thermal conductivity of fluid, B.t.u./ (hr.ft. °F.)

- k_s = thermal conductivity of solid particle, B.t.u./ (hr.ft. °F.)
 ΔL = thickness of an element of the model (Figure 8) which is repeated throughout the bed, ft.
 L = Length (axial distance) of packed bed, ft.
 l_s = equivalent length of path for heat transfer by conduction in the particle, ft.
 l_e = equivalent length of path for heat transfer by conduction through the fluid between particles, ft.
 n = number of contact points with other particles on the hemispherical surface of a sphere.
 Q = heat flow rate, B.t.u./hr.
 r = radial distance in packed bed, measured from center, ft.
 T = temperature, °F.

Greek Symbols

- α = $\phi + \gamma \frac{k_p}{k_s}$
 γ = l_s/D_p
 ϕ = l_e/D_p
 ϵ = actual void fraction of bed
 ϵ^* = so-called void fraction defined by Equation (3)
 θ_s = angle defining the boundary of heat flow through fluid adjacent to a contact point, reference 5 and Equation (6)

LITERATURE CITED

1. Lucken, A., *Forsch. Gebiete Ingenieurw.*, **133**, No. 153, p. 16 (1932).
2. Kannuluick, W. G., and L. H. Martin, *Proc. Royal Soc. (London)*, **A141**, 144 (1933).
3. Kimura, M., *Chem. Eng. (Japan)*, **21**, 472 (1957).
4. Kling, G., *Forsch. Gebiete Ingenieurw.*, **9**, No. 28, p. 82 (1938).
5. Kunii, Daizo, and J. M. Smith, *A.I.Ch.E. Journal*, **6**, 71 (1960).
6. *Ibid.*, **7**, 29 (1961).
7. Preston, F. W., Ph.D. thesis, Pennsylvania State Univ., State College, Pennsylvania (1957).
8. Schumann, T. E. W., and V. Voss, *Fuel*, **13**, 249 (1934).
- 8a. Singer, E., Private communication.
9. Skelly Oil Company, Private communication.
10. Smith, W. O., P. D. Foote, and P. F. Busang, *Phys. Rev.*, **34**, 1271 (1929).
11. Waddams, A. L., *J. Soc. Chem. Ind.*, **63**, 337 (1944); *Chem. & Ind. (London)*, **22**, 206 (1944).
12. Weiniger, J. L., and W. G. Schneider, *Ind. Eng. Chem.*, **43**, 1229 (1951).
13. Wilhelm, R. H., W. C. Wynkoop, and D. W. Collier, *Chem. Eng. Progr.*, **44**, 105 (1948).
14. Yagi, Sakae, and Daizo Kunii, *Chem. Eng. (Japan)*, **18**, 576 (1954); *A.I.Ch.E. Journal*, **3**, 373 (1957).

Manuscript received April 20, 1961; revision received October 16, 1961; paper accepted October 17, 1961.

TABLE 2. RANGE OF CONDITIONS FOR DATA PRESENTED IN FIGURE 9

Solids	Average particle diameter—in.	Void fraction	Investigator	Literature cited
Steel spheres	0.15	0.38	Kling	(4)
Steel spheres	0.157 to 0.219	0.38 to 0.39	Waddams	(11)
Calcite	0.098 to 0.563	0.46 to 0.49	Waddams	(11)
Silicon carbide	0.00236 to 0.0216	0.41 to 0.43	Kannuluick	(2)
Diphenyl amine	0.00106	0.51	Kannuluick	(2)
Copper	0.0059 to 0.0068	0.38 to 0.39	Preston	(7)
Silica	0.00504 to 0.096	0.41 to 0.44	Preston	(7)
Glass	0.0132 to 0.089	0.41 to 0.43	Preston	(7)
Lead	0.0132 to 0.0179	0.40 to 0.42	Kimura	(3)
Calcite	0.056 to 0.112	0.45 to 0.46	Kimura	(3)
Lead	0.103	0.40	Schumann and Voss	(8)
Coal		0.44	Schumann and Voss	(8)